Eur. Phys. J. A **14**, 371–376 (2002)
DOI 10.1140/epja/i2002-10007-y

THE EUROPEAN PHYSICAL JOURNAL A

Energy spectra and angular distribution of projectile-like fragments in 84 MeV $^{12}C + ^{169}Tm$

S. Sodaye[1], K. Sudarshan[1], B.S. Tomar[1,a], A. Goswami[1], S. Mukherjee[2], and K. Mahata[3]

[1] Radiochemistry Division, Bhabha Atomic Research Centre, Mumbai 400 085, India
[2] School of Studies in Physics, Vikram University, Ujjain 456010, India
[3] Nuclear Physics Division, Bhabha Atomic Research Centre, Mumbai 400 085, India

Received: 13 March 2002
Communicated by W. Henning

Abstract. Kinetic-energy spectra and angular distribution of projectile-like fragments have been measured in the reaction of 84 MeV ^{12}C on ^{169}Tm, using the surface barrier silicon-based ΔE-E telescopes. The fragments close to the projectile show typical spectra of quasi-elastic transfer reactions, which were found to be in agreement with the calculations based on the direct surface transfer reaction model. A significant cross-section of fast alpha-particles was found at forward angles, reminiscent of incomplete fusion reactions, which could be explained in terms of the direct surface transfer reaction model after taking into account the level density of continuum states in the heavy reaction product. The results have been explained in terms of the continuous evolution of the reaction mechanism as a function of the mass transfer.

PACS. 25.70.Gh Compound nucleus – 25.70.Jj Fusion and fusion-fission reactions

1 Introduction

The mechanism of the formation of projectile-like fragments (PLFs) in heavy-ion reactions has been of considerable interest for the past three decades. While the PLFs having Z and A close to the projectile are formed in quasi-elastic transfer (QET) reactions, those far removed from projectile were explained in terms of incomplete fusion (ICF) or massive transfer reactions. On the other hand, deep-inelastic collisions (DIC) are manifested in all types of PLFs as the low-energy tails extending down to the exit channel Coulomb barrier. The quasi-elastic transfer reactions are characterised by bell-shaped angular distributions having a maximum near the grazing angle while, the ICF reactions are characterised by forward-peaked angular distributions. The energy spectra of ejectiles formed in QET and ICF are found to be peaked at $Q_{\rm opt}$ [1].

Among the various ICF channels, emission of fast alpha-particles is known to constitute a major fraction of the ICF cross-section [2]. While extensive studies on measurement of these fast alpha-particles have been carried out to understand the mechanism of ICF reactions, a complete theoretical understanding of the underlying mechanism is yet to emerge. Britt and Quinton [3] were the first to observe the fast alpha-particles in the bombardment of ^{197}Au and ^{209}Bi by ^{12}C, ^{14}N and ^{16}O projectiles at 10.5 MeV/nucleon. Subsequently Galin *et al.* [4] termed these reactions, leading to fast alpha-particles, as incomplete fusion reactions. However, major advances in the study of these ICF reactions took place after the work of Inamura *et al.* [5] wherein exclusive measurements of forward-peaked alpha-particles in coincidence with the discrete gamma-rays of the evaporation residues were made.

Several models were proposed to explain the mechanism of these ICF reactions. Wilczynski *et al.* [1] proposed the sum rule model according to which the various ICF channels are localised in the angular-momentum space above the critical angular momentum for complete fusion (CF) of the projectile and target. The model was successful in explaining the cross-section of all the PLFs at beam energies above 10 MeV/nucleon. The break-up fusion model proposed by Udagawa and Tamura [6] explained the shape of energy spectra and angular distributions of fast alpha-particles formed in ICF reactions, though the absolute cross-sections could not be deduced.

During the past few years there has been a renewed interest in the mechanism of these reactions after the observation of ICF reactions at beam energies as low as 5 MeV/nucleon [7–10]. This became evident from the measurement of excitation functions and recoil range distribution (RRD) of evaporation residues (ERs) [11–13] and by the measurement of the kinetic-energy spectra and angular distribution of projectile-like fragments (PLFs) [14–16]. These observations could not be explained in terms

[a] e-mail: bstomar@apsara.barc.ernet.in

of the sum rule model as the critical angular momentum at such low beam energies is very close to the maximum angular momentum, thus precluding the existence of a sizable angular-momentum window for ICF. In fact, it has been suggested that ICF may be competing with CF at beam energies just above the Coulomb barrier [9].

Most of the ICF studies have been confined to low-Z ($\leqslant 10$) projectile-induced reactions on targets of medium mass ($A \sim 100$). There have been very few studies with heavier targets. One advantage of using heavier targets is that the evaporation of alpha-particles from the compound nucleus (CN) becomes less probable because of the high emission barrier, thereby making it easier to distinguish the ICF alpha-particles from the CF alpha-particles. With this in view, we undertook studies on incomplete fusion reactions at beam energies around 5–8 MeV/nucleon in the reactions of low-Z heavy ions on rare-earth targets [17,18]. In these studies, cross-sections for different ICF products were obtained from the RRDs of the evaporation residues. In the present paper, we report the results of our measurements on projectile-like fragments (PLFs) in 84 MeV $^{12}\mathrm{C} + {}^{169}\mathrm{Tm}$. The measured kinetic-energy spectra and angular distributions of PLFs have been compared with those calculated using the diffractional surface transfer reaction model. Elastic scattering measurements were also carried out to obtain the optical model parameters for the system, grazing angular momentum and the total reaction cross-section.

2 Experimental

The experiments were carried out at the BARC-TIFR Pelletron accelerator facility at Mumbai. Self-supporting thulium metal targets, having thickness around 1 mg/cm^2, were bombarded with ^{12}C beam of energy 84 MeV. The PLFs were detected using two surface barrier silicon-based ΔE-E telescopes. In both the telescopes, the ΔE detectors were 30 μm thick and the E detectors were 2 mm thick. The solid angle subtended by both telescopes was 1.62 msr. Angular distributions of PLFs were measured in the range of 20°–168° in steps of 5° at forward angles and 10° at backward angles with respect to the beam direction. The angular resolution of the detectors was 2.6°. The energy calibration of the telescopes was carried out using elastically scattered ^{7}Li beam. A 250 μm silicon surface barrier detector kept at 20° with respect to the beam direction was used to monitor Rutherford cross-section, which was used for the absolute normalisation of PLF cross-sections. The scattered energy of ^{7}Li was varied in the range of 24.8–49.8 MeV. The elastic peaks in the case of the $^{12}\mathrm{C} + {}^{169}\mathrm{Tm}$ reaction measured at different forward angles were also used for energy calibration of the telescopes. The signals from E and ΔE detectors of each telescope were fed to two analog-to-digital converters (ADCs), whose inputs were gated so as to receive only events having a valid pair of ΔE and E signals. The data were stored as two-dimensional spectra using a CAMAC-based multiparameter data acquisition system. Subsequently, the data were transformed into two parameter maps of total energy, $E + \Delta E$, *versus* a parameter characteristic of the particle defined as

$$PI = [(E + \Delta E)^b - E^b]^a , \quad (1)$$

where the coefficients a and b were taken as 1 and 1.67, respectively. The backward-angle alpha spectra showed a low-energy component due to oxygen impurity in the target. In order to confirm this, an alpha spectrum for the 63 MeV $^{16}\mathrm{O} + {}^{12}\mathrm{C}$ reaction was recorded at an angle of 45°, with respect to the beam direction, in a separate experiment. The thickness of carbon target was 80 μg/cm^2. The beam energy of 63 MeV was chosen to get the same recoil velocity of ^{28}Si as in 84 MeV ^{12}C on ^{16}O. The low-energy component obtained in 84 MeV $^{12}\mathrm{C} + {}^{169}\mathrm{Tm}$ was found to be in good agreement with the alpha spectrum for 63 MeV $^{16}\mathrm{O} + {}^{12}\mathrm{C}$, showing the origin of this component.

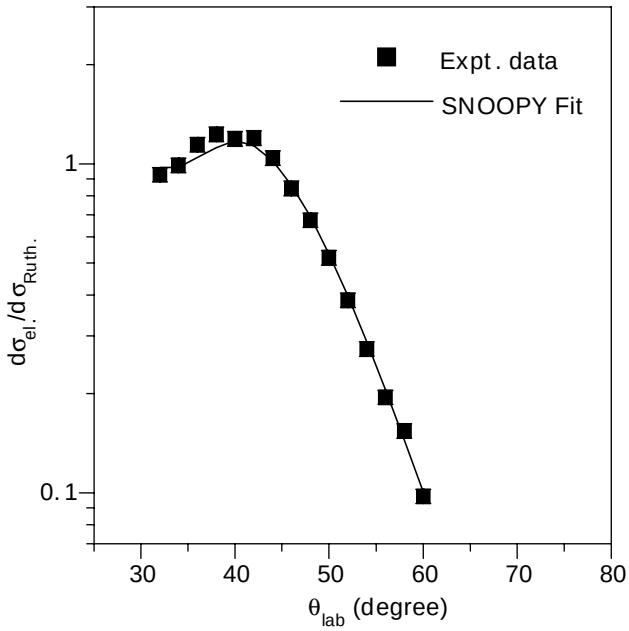

Fig. 1. Elastic-scattering angular distribution for $^{12}\mathrm{C} + {}^{169}\mathrm{Tm}$ at 84 MeV. The solid line represents the optical-model fit to the data using SNOOPY.

3 Results and discussion

3.1 Elastic scattering

Figure 1 shows the elastic-scattering data plotted as a function of θ_{lab}. In order to get the optical-model parameters for the reaction, the measured elastic-scattering angular distribution was fitted using the SNOOPY code [19]. The smooth curve represents the fitted curve. The optical-model parameters were obtained as $V_0 = 35.06$ MeV, $R_0 = 1.138$ fm, $a_0 = 0.819$, $W_0 = 28.02$ MeV, $R_{\mathrm{w}} = 1.224$ fm and $a_{\mathrm{w}} = 0.591$. The quarter point angle $\theta_{1/4}$ (CM) was found to be 55°. The grazing angular momentum (l_{g}) and reaction cross-section calculated from the quarter point angle were found to be $47\,\eta$ and 1598 mb, respectively. The fusion cross-section ((σ_{CF}) for 84 MeV $^{12}\mathrm{C} + {}^{169}\mathrm{Tm}$,

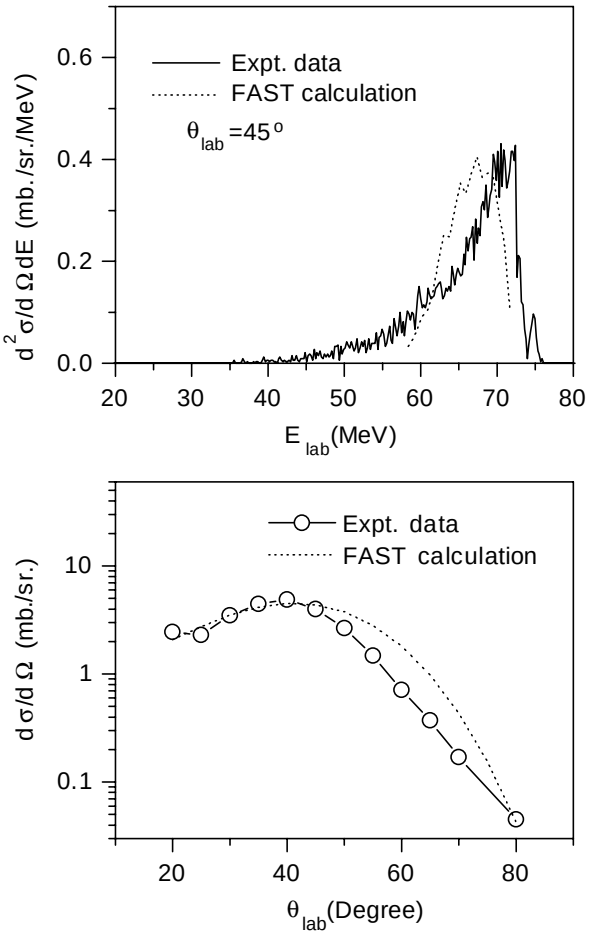

Fig. 2. Kinetic-energy spectrum at $\theta_{\rm lab} = 45^\circ$ (top) and angular distribution (bottom) of boron in the reaction of $^{12}\mathrm{C} + {}^{169}\mathrm{Tm}$ at 84 MeV. Dotted lines represent the calculations using the FAST code.

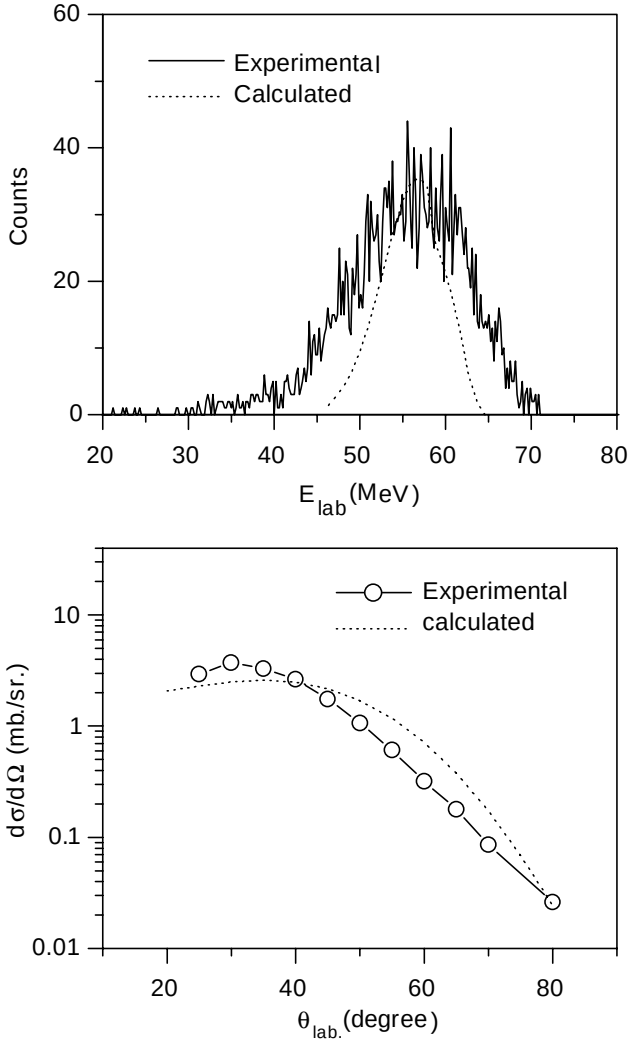

Fig. 3. Kinetic-energy spectrum at $\theta_{\rm lab} = 40^\circ$ (top) and angular distribution (bottom) of beryllium in the reaction of $^{12}\mathrm{C} + {}^{169}\mathrm{Tm}$ at 84 MeV. Dotted lines represent the calculations using the FAST code.

calculated using the Bass formula [20], was found to be 1171 mb. The critical angular momentum ($l_{\rm cr}$) corresponding to the fusion cross-section was found to be $39\,\eta$. Considering the peripheral nature of collisions leading to ICF, angular-momentum values between $39\,\eta$ and $47\,\eta$ are expected to be associated with ICF, inelastic scattering as well as transfer reactions.

3.2 Boron and beryllium data

Figure 2 shows the kinetic-energy spectrum at $\theta_{\rm lab} = 45^\circ$, and the angular distribution of boron. The corresponding data for beryllium are shown in fig. 3. The angular distribution of boron shows a maximum at $\theta_{\rm lab} = 40^\circ$ and that of beryllium shows a maximum at $\theta_{\rm lab} = 35^\circ$. In both these cases the mass resolution of the PLF data was not adequate to resolve the spectra of individual isotopes.

3.3 Alpha spectra

The measured kinetic-energy spectra of alpha-particles were transformed into the center-of-mass (CM) system using the standard kinematic relationships. The CM spectra of alpha-particles emitted in the backward angle show two components. The low-energy component was found similar to that observed in the reaction of 63 MeV $^{16}\mathrm{O} + {}^{12}\mathrm{C}$ indicating that this tail is due to the oxygen impurity in the target. This low energy tail was fitted to a Maxwellian function, which was subtracted from the observed data to obtain the CF alpha spectra. A typical backward-angle spectrum showing different components is shown in fig. 4. The dotted curve represents the CF alpha spectrum obtained from the CASCADE code [21] and normalised with the measured CF spectrum. As seen from the figure, the calculated spectrum agrees with the measured CF spectrum quite well. From these backward-angle data, angular distribution of alpha-particles emitted in CF was generated, assuming the forward-backward symmetry.

The measured forward-angle alpha-particle spectra were found to be complex, with contribution from alpha-

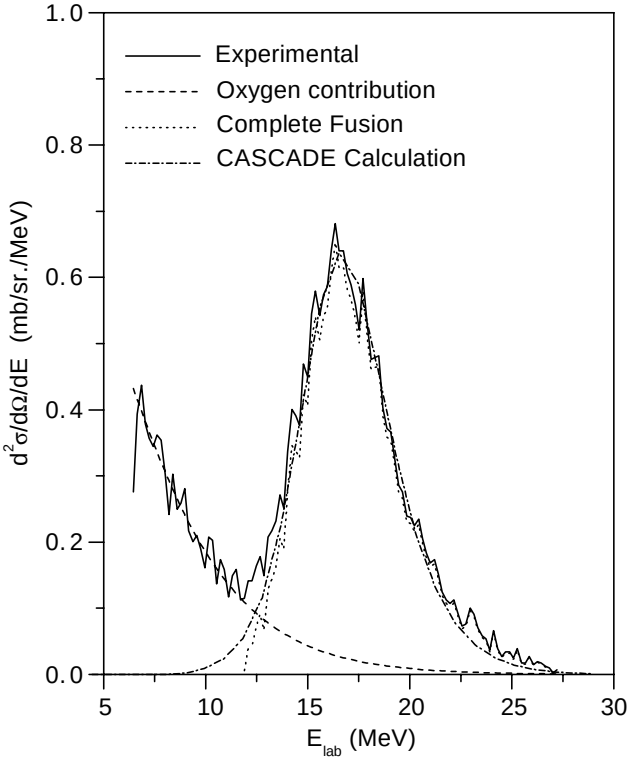

Fig. 4. Alpha-particle spectrum at $\theta_{\rm lab} = 130^\circ$ in the reaction of 84 MeV ^{12}C on ^{169}Tm.

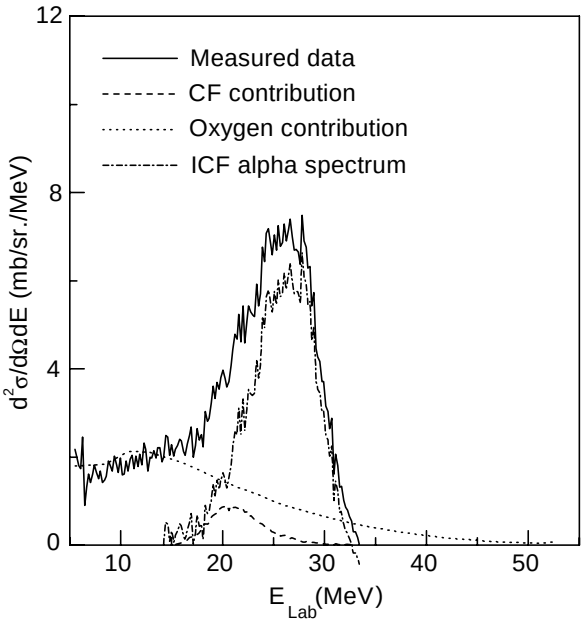

Fig. 5. Kinetic-energy spectrum of alpha-particles at $\theta_{\rm lab} = 40^\circ$ in the reaction of 84 MeV ^{12}C on ^{169}Tm.

particles emitted in CF, ICF as well as those coming from 84 MeV ^{12}C + ^{16}O reaction. Figure 5 shows a typical alpha-particle spectrum for forward angles.

The CF alpha spectrum at forward angles was obtained from the backward-angle alpha spectra after correcting for the angular distribution. This component is shown as a dashed curve in fig. 5. The low-energy tail in the alpha spectrum is indicative of the presence of oxygen impurity in the target, as was observed clearly in the backward-angle spectra. This spectrum was simulated using the CASCADE code and is shown as a dotted line in fig. 5. As seen from fig. 5, the CF alpha-particles and alpha-particles from oxygen impurity in the target constitute a small fraction of the total alpha-particles observed in the forward angles, showing the abundance of ICF alpha contribution in these spectra. Subtraction of these two components from the measured spectrum leaves a high-energy ICF component with a peak energy close to the beam velocity, which is shown as a dash-dotted curve in fig. 5. Figure 6 shows the angular distribution of alpha-particles from ICF reactions obtained by integrating the kinetic-energy spectra. The angular distribution ($d\sigma/d\Omega$) was integrated over the angular range of the measurement, that is, 20°–80°, to obtain the cross-section of alpha-particles formed in ICF. The ICF alpha-particle cross-section was found to be 90 ± 9 mb, which is in agreement with that obtained from RRD data [18].

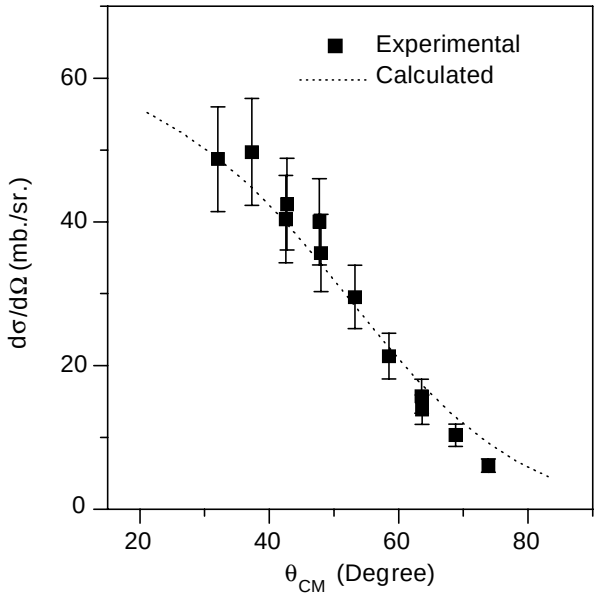

Fig. 6. Angular distribution of fast alpha-particles in the ^{12}C + ^{169}Tm reaction at 84 MeV. The dotted line is calculated using the FAST code.

3.4 Direct surface transfer reaction model calculations for PLFs

In order to investigate the mechanism of reaction leading to different projectile-like fragments, the kinetic-energy spectra and angular distribution of PLFs were calculated in the framework of the diffractional model for surface transfer reactions based on the DWBA formalism of Mermaz [22] using the code FAST.

The double differential cross-section to the continuum states, according to the formalism of Mermaz *et al.* [22],

is given by the formula

$$\frac{\mathrm{d}^2\sigma}{\mathrm{d}\Omega \mathrm{d}E_\mathrm{f}} = \sum_{J_1,J_2} \sum_{J_1-J_2}^{J_1+J_2} \int_0^{E_0^*} \rho_1(E_0^* - E_2^*, J_2) \cdot \rho_2(E_2^*, J_2)\sigma(E_\mathrm{f}, \theta, L_\mathrm{T})\mathrm{d}E_2^* \,. \quad (2)$$

The indices 1 and 2 represent the PLF and the residual nucleus, respectively, $\sigma(E_\mathrm{f}, \theta, L_\mathrm{T})$ is the reduced transfer cross-section given by the diffractional model of Blair, Austern and Hahne. E_f is the final CM kinetic energy of the ejectile at angle θ and L_T is the transferred angular momentum. $\rho(E^*, J)$ is the spin-dependent level density of the excited nuclei defined as

$$\rho(E^*, J) = [\rho(E^*)]\frac{(2J+1)}{2\sigma^3\sqrt{2\pi}} \cdot \exp\left[-J(J+1)/2\sigma^2\right], \quad (3)$$

where, $\rho(E^*)$ is the level density of particles and holes in the PLF and residual nucleus with respect to the projectile and the target nuclei. σ is the spin cut-off parameter. For the level density of particle and hole states, the formula of Williams [23] is used. E_0^* is the total excitation energy for the residual nucleus and the PLF. In the present calculations the excitation energy of the PLF was restricted to 10 MeV, so as to preclude particle emission from the excited PLFs.

The model was used to calculate the kinetic-energy spectra and angular distributions of PLFs (boron and beryllium) which are expected to be formed in quasi-elastic transfer reactions. The input parameters in the calculations are the radius constant (R_0), the diffusivity (d) and the phase angle $\Delta\theta$, which is the difference between the Coulomb and the nuclear rainbows. The set of parameters as recommended by Mermaz *et al.* [22] for lower beam energies, namely 1.5, 0.25 and -0.4 for R_0, d_0 and $\Delta\theta$, respectively, was used in the present calculations. As the spectroscopic form factors of the continuum states could not be supplied in the code, the calculation did not give the absolute cross-sections. The calculated kinetic-energy spectra and angular distributions were normalised to the experimental data and are shown as dotted lines in the respective figures. The good agreement between calculated and experimental kinetic-energy spectra and angular distribution of boron and beryllium fragments indicates the formation of these PLFs in quasi-elastic transfer reactions.

The above set of input parameters were used to calculate the energy spectra and angular distribution of fast alpha-particles. The calculations reproduced the angular distribution of the alpha-particles as shown in fig. 6, but the mean kinetic energy was found to be higher than the experimental mean value. This indicates that the formation of these fast alpha-particles involves large overlap between the projectile and the target leading to a higher excitation energy in target-like fragments. Therefore, the level density formalism of Gilbert and Cameron [24] was used in the FAST code to calculate the alpha-particle spectra. Similar approach was used by Mermaz *et al.* [25] while

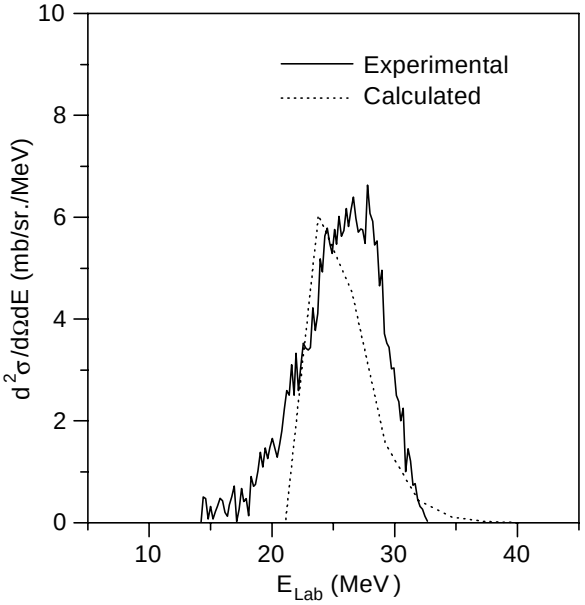

Fig. 7. Kinetic-energy spectrum of incomplete-fusion alpha-particles at $\theta_\mathrm{lab} = 40°$ in the reaction of 84 MeV ^{12}C on ^{169}Tm. The dotted line is calculated using the FAST code (see text for details).

calculating the spectra of PLFs far removed from projectile. The level density parameter (a) was varied in the range of $A/10$ to $A/6\,\mathrm{MeV}^{-1}$. The agreement was found to be the best with $a = A/7\,\mathrm{MeV}^{-1}$. This is understandable in view of the deformed structure of the nuclei around the mass number 170. The calculated spectrum is shown in fig. 7 for $\theta_\mathrm{lab} = 40°$. A reasonable agreement between the experimental and calculated ICF alpha spectra suggests the use of Gilbert and Cameron level density formalism to be more appropriate at higher mass transfer. Thus, by taking into account the level density of the continuum states in the residual nuclei it is possible to explain the energy spectra of the PLFs formed in ICF reactions.

4 Conclusion

In the present study, the kinetic-energy spectra and angular distribution of PLFs, including alpha-particles were measured at 84 MeV ^{12}C + ^{169}Tm reaction. The alpha-particle spectra at forward angles, when corrected for the contribution from CF alpha-particles and that from oxygen impurity was found to have a sizable beam velocity component having a forward-peaked angular distribution. The total cross-section of ICF α-particles agrees with that obtained in our earlier study based on recoil range distribution of ERs. Boron and beryllium fragments show left-skewed kinetic-energy spectra and side-peaked angular distribution, reminiscent of quasi-elastic transfer reactions. This is further corroborated by the calculation of kinetic-energy spectra and angular distribution using the direct surface transfer reaction model. In the case of alpha-particles, a better agreement between the experimental spectra and calculated spectra is obtained with the

level density of continuum states given by the formalism of Gilbert and Cameron.

Authors thank S.B. Manohar Head, Radiochemistry Division, Dr. S. Kailas, Head, Nuclear Physics Division, and Dr. A.V.R. Reddy for their keen interest and encouragement during this work. They also thank Dr. A. Navin for his suggestions during the experiment. Thanks are due to the operation crew of Pelletron Accelerator Facility, Mumbai for their cooperation during the experiment.

References

1. J. Wilczynsky, K. Siwek-Wilczynska, J. Van Driel, S. Gonggrijp, D.C.J.M. Hageman, R.V.F. Janssens, J. Lukasiak, R.H.siemssen, S.Y. Van der Werf, Nucl. Phys. A **373**, 109 (1982).
2. Ch. Ngo, Prog. Part. Nucl. Phys. **16**, 139 (1985).
3. H.C. Britt, A.R. Quinton, Phys. Rev. **124**, 877 (1961).
4. J. Galin, B. Gatty, M.lefort, J. Peter, X. Tarrago, R. Basile, Nucl. Phys. A **159**, 161 (1970).
5. T. Inamura, M. Ishihara, T. Fakuda, T. Shimoda, H. Hiruta, Phys. Lett. B **68**, 51 (1977).
6. T. Udagawa, T. Tamura, Phys. Rev. Lett. **45**, 1311 (1980).
7. I. Tserruya, V. Steiner, Z. Fraenkel, P. Jacobs, D.G. Kovar, W. Henning, M.F. Vineyard, B.G. Glagola, Phys. Rev. Lett. **60**, 14 (1988).
8. D.J. Parker, J. Asher, T.W. Conlon, N. Naquib, Phys. Rev. C **30**, 143 (1984).
9. D.J. Parker, J.J. Hogan, J. Asher, Phys. Rev. C **35**, 161 (1987)
10. B.S. Tomar, A. Goswami, A.V.R. Reddy, S.K. Das, P.P. Burte, S.B. Manohar, B. John, Phys. Rev. C **49**, 941 (1994).
11. B. Bindukumar, S. Mukherjee, S. Chakrabarty, B.S. Tomar, A. Goswami, S.B. Manohar, Phys. Rev. C **57**, 743 (1998).
12. B. Bindukumar, Anil Sharma, S. Mukherjee, S. Chakrabarty, P.K. Pujari, B.S. Tomar, A. Goswami, S.B. Manohar, S.K. Datta, Phys. Rev. C **59**, 2923 (1999).
13. Anil Sharma, B. Bindukumar, S. Mukherjee, S. Chakrabarty, B.S. Tomar, A. Goswami, S.B. Manohar, J. Phys. G: Nucl. Phys **25**, 2289 (1999).
14. B.S. Tomar, A. Gosawmi, G.K. Gubbi, A.V.R. Reddy, S.B. Manohar, Phys. Rev. C **58**, 3478 (1998).
15. A. Yokoyama, T. Saito, H. Baba, K. Hata, Y. Nagame, S. Ichikawa, S. Baba, A. Shinohara, N. Imanishi, Z. Phys. A **332**, 71 (1989).
16. M. Lunardon, C. Merigilano, G. Viesti, D. Fabris, G. Nebbia, M. Cinausero, G.de Angelis, E. Fernea, E. Fiorreto, G. Prete, A. Brondi, G. La Rana, R. Moro, A. Prinipe, E. Vardaci, N. Gelli, F. Lucarelli, P. Pavan, D.R. Napoli, G. Vedovato, Nucl. Phys. A **652**, 3 (1999).
17. Anil Sharma, B. Bindukumar, S. Mukherjee, S. Chakrabarty, B.S. Tomar, A. Goswami, S.B. Manohar, Pramana, J. Phys. **54**, 355 (2000).
18. S. Chakrabarty, B.S. Tomar, A. Goswami, G.K. Gubbi, S.B. Manohar, Anil Sharma, B. Bindukumar, S. Mukherjee, Nucl. Phys. A **678**, 355 (2000).
19. P. Schwandt, Indiana University Cyclotron Facility, SNOOPY Computer Programme: Optical Potential Model Code for Elastic Scattering Analysis, Indiana University Cyclotron Report (1988).
20. R. Bass, Nucl. Phys. A **231**, 45 (1974).
21. F. Puhlhofer, Nucl. Phys. A **280**, 267 (1977).
22. M.C. Mermaz, R. Dayras, J. Barrette, B. Berthier, D.M. De Castro Rizzo, O. Cisse, R. Legrain, A. Pagano, E. pollacco, H. Delgrage, W. Mittig, B. Heusch, G. Langano, A. Palmeri, Nucl. Phys. A **441**, 129 (1985).
23. F.C. Williams jr., Nucl. Phys. A **166**, 231 (1971).
24. A. Gilbert, A.G.W. Cameron, Can. J. Phys. **43**, 1446 (1965).
25. M.C. Mermaz, J. Barrette, H.E. Wegner, Phys. Rev. C **24**, 2148 (1981).